JRC Technical Notes

IMAGE-2006 Mosaic: Product Description

Pierre Soille and Conrad Bielski

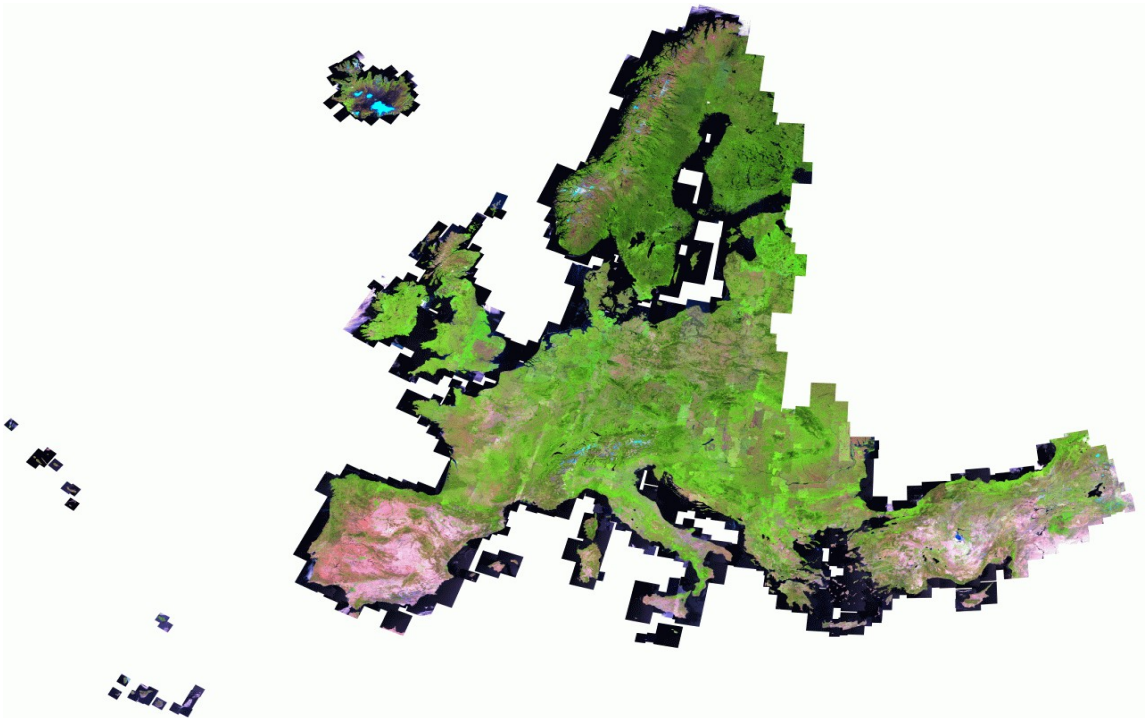

EUR 23636 EN

JRC EUROPEAN COMMISSION

ies Institute for Environment and Sustainability

The mission of the Institute for Environment and Sustainability is to provide scientific-technical support to the European Union's Policies for the protection and sustainable development of the European and global environment.

European Commission
Joint Research Centre
Institute for Environment and Sustainability
Spatial Data Infrastructures Unit

Contact information
Address: via E. Fermi 2749, I-21027 Ispra (Italy)
E-mail: Pierre.Soille@jrc.ec.europa.eu
Tel.: int+39-0332 785 068
Fax: int+39-0332 786 325

http://ies.jrc.ec.europa.eu/
http://www.jrc.ec.europa.eu/

JRC 49568

EUR 23636 EN
ISBN 978-92-79-20960-4
ISSN 1831-9424
doi:10.2788/51244

Luxembourg: Publications Office of the European Union, 2011

IMAGE-2006 Mosaic: Product Description

Pierre Soille and Conrad Bielski
COSIN Action
IES-Spatial Data Infrastructures Unit

December 23, 2008

Abstract

This report describes the IMAGE-2006 mosaic products. Each product consists of a range of information layers grouped into three categories: base layers, mosaic layers, and quality layers. A mosaic product is available for each coverage and data/country region of interest combination.

Contents

1 Introduction

The mosaicing methodology described in [5, 2, 8] was applied to the IMAGE-2006 data sets to generate a series of mosaics. Each mosaic is supplemented with a range of additional information layers of interest to subsequent information extraction. Actually, the core information layer does not contain the multispectral imagery but simply the labelled decision regions together with the correspondence table indicating which image should be selected for each label value of the decision regions. Hence, the determination of the origin of the pixel values of any pixel of the mosaiced multispectral imagery is straightforward. Furthermore, the decision regions can be directly mapped, thanks to appropriate look-up-tables, to sensor type, year of acquisition, or any other attribute varying from one image to another.

This report is organised as follows. A description of each type of each stored information layer is given in Sec. 2. The mosaics of coverages 1 and 2 are described in Secs. 3 and 4 respectively. A brief conclusion is presented in Sec. 5.

2 Information layers

The produced mosaics are organised in directories indicating the coverage name and type of ROI used (either DROI or CROI). Images for a given coverage were retrieved from the reference coverage by searching for all header files containing this coverage in their `data_Set` field, see sample header file in [7, Fig. 5]. Indeed, contrary to image searches conducted directly on coverage 1 or 2, image searches conducted on the reference coverage always lead a set of unique images because multiple deliveries of the same scene were merged when creating the reference coverage, see [7, Sec. 6]. To emphasise that images were retrieved from the reference coverage, the string `REF` is included in the directory name of the mosaic products. For example, `2006_REF-MOS-COV1-CROI` corresponds to the mosaic product of all imagery of the first coverage retrieved from the reference coverage and calculated on the basis of CROIs.

Each mosaic is then stored in directories following the level 18 of the European Reference Grid [1]. Each level 18 (square) tile covers a region of 250,000 km^2 stored in a raster file of $20{,}000 \times 20{,}000$ pixels at a spatial resolution of 25 m. For instance, Switzerland falls fully in the level 18 tile named `42-C`. For convenience, the chosen convention for naming level 18 information layers departs somewhat from the specifications put forward in [11]. The `date-time` field has been set to the median of the dates of the whole input imagery so that the same value is used for all tiles[1]. The centre pixel field has been substituted by the level 18 tile name itself, e.g., `42-C`. The `type` sub-field of the `type-identifier` field is set to `MXT` to emphasise that the tiles consist of a mixture of more than one image.

Although all stored layers appear together in a given level 18 directory, they can be naturally grouped into three categories: (i) base layers, (ii) mosaic layers, and (iii) quality layers. Each category is described in a separate section hereafter.

[1] According to [11], it would be more precise to use the weighted median of the dates of the image pieces used for creating each tile.

2.1 Base layers

Base layers are information layers that were generated independently of the mosaicing results using point-wise operations between the input imagery, their ROIs, or their cloud masks. They consist of 4 layers:

1–2. point-wise minimum (`date_MXT_CM-INFn_tile.tif`) and point-wise maximum (`date_MXT_CM-SUPn_tile.tif`) compositions of all input imagery with one file per band, `n` referring to the band number, the operations being restricted to the ROI extent considered during mosaicing (either DROI or CROI). The DN values of the pixels correspond to Top Of the Atmosphere (TOA) values rescaled between 0 and 250. The value 255 is reserved for no data value. These GeoTIFF files are of interest for visual quality control of the mosaic as advocated in [6]. For instance, a cloud appearing in the point-wise minimum composition indicates that this region is always covered by clouds so that they will also be visible in any mosaic produced with the same set of input imagery. Similarly, a region appearing as a cloud shadow in the point-wise minimum composition will always appear as such in a mosaic based on the same set of input imagery.

3. point-wise addition of cloud masks expanded in the direction opposite to the sun azimuth angle and restricted to the ROI extent considered during mosaicing (either DROI or CROI). Resulting aggregated cloud/shadow masks are stored int he file `date_MXT_CLSH_tile.tif`. The cloud masking algorithm is detailed in [6]. Beware that the North direction is pointing upwards only for pixels centred on the meridian corresponding to the LAEA projection centre (i.e., 10^o East). The actual direction of the North of was calculated for the centre pixel of each scene and used for all pixels of the considered scene.

4. degree of overlap images (`date_MXT_GLVL_tile.tif`). This GeoTIFF file indicates the number of input images that is covering any given pixel. Hence, pixels set to 0 in this image are not covered by the input imagery. The maximum number of overlap levels is equal to 255 (maximum value for an unsigned byte integer).

2.2 Mosaic layers

The second category of layers holds the main outputs of the mosaicing procedure. It contains 4 main items:

1. mosaic of the input images given the produced decision regions, one file per band (`date_MXT_IP-BnOC_tile.tif`), `n` referring to the band number. The DN values of these GeoTIFF files correspond to Top Of the Atmosphere (TOA) values rescaled between 0 and 250. The value 255 is reserved for no data value.

2. labelled decision regions (`date_MXT_BASE_tile.tif`). These GeoTIFF files indicate from which image the value of each pixel should originate from. Indeed, there is a one-to-one correspondence between the label values and the input images. The correspondence is given in the ASCII file `tile.tif_list.txt` described hereafter (item number 3). The pixel data

type used for storing the decision regions is an unsigned two byte integer. The maximum label value is equal to 65534, the value 65535 being reserved for no data. The labelled decision regions are the core of the mosaic since they indicate where the cut between overlapping images should take place and which part of the images should be thrown away;

3. lists of GeoTIFF files (`tile.tif_list.txt`). These two column ASCII files contain the correspondence table between labels of the decision regions and the file name of the updated ROI of the input images they correspond to. A typical line of these files looks like:

   49 22-B/20060723-1124_IL3_IM-UROI_2966422035-AC.tif

   That is, the image of the reference coverage uniquely defined by the date-time, sensor, and centre pixel fields of the indicated GeoTIFF file name should be used for all decision regions labelled with the value 49.

4. a series of look-up-tables (LUTs) mapping the label values to relevant information relative to their corresponding images. These LUTS are stored in ASCII files following the ENVI™ `dsr` (density slice range) format. The following LUTs are available:

   (a) sensor LUT mapping each label value to the sensor type of its corresponding image (`date_tile_sensor.dsr`). Sensors are represented with the following colours: red for SPOT-4, green for SPOT-5, and blue for IRS-LISS III.

   (b) year LUT mapping each label value to the year of acquisition of the corresponding image (`date_tile_year.dsr`). The following colour codes are used: red for 2005, green for 2006, and blue for 2007;

   (c) month LUT mapping each label value to the month of acquisition of its corresponding image (`date_tile_month.dsr`). Colour codes for months are derived from the colour wheel setting January to blue, February to cyan blue, Mars to cyan, April to cyan green, May to green, June to yellow green, August to orange, September to red, October to pink, November to magenta, and December to violet.

   (d) week in year LUT mapping each label value to the week of acquisition of its corresponding image (`date_tile_week.dsr`). The colour wheel is also used for mapping a specific week to a colour, starting with blue for the first week and using violet for the last week of the year (colour wheel).

Because the label values are unique across all tiles, only one set of LUTs is saved for all tiles rather than storing subsets of these LUTs for each tile. The LUTs are therefore stored in a sub-directory named `ALL`, appearing at the same level as the tiles. This directory also holds a file containing the correspondence between label values and image names for all input imagery. It is named `UROI_list.txt`

2.3 Quality layers

The third category of layers contains files useful for a spatial representation of quantitative measurements of the geometric and radiometric consistency between adjacent decision regions of the mosaic. This is achieved by setting the

boundary pixels of the decision regions to appropriate values. These values originate from the comprehensive relative and geometric consistency measurements detailed in [9]. The quality layers contain 4 main items:

1–2. two images giving, for each pixel of the support of the morphological gradient [3] of the decision regions, the lowest (resp. greatest) label value in a 4-neighbourhood. These values are obtained by multiplying the support of the morphological gradient by the erosion (resp. dilation) of the labelled decision regions with a elementary diamond-shaped structuring element [4]. The images are stored in the files `date_MXT_BASE-ERO_tile.tif` (resp. `date_MXT_BASE-DIL_tile.tif`).

3. a two dimensional LUT stored a TIFF image `date_ERODIL_LUT_HST_tile.tif`. The value at coordinates x-y of this image indicates the number of pixels that have the value x in the image `date_MXT_BASE-ERO_tile.tif` and, at the same time, the value y in the image `date_MXT_BASE-DIL_tile.tif`. It corresponds therefore to the two-dimensional frequency distribution using as input the 'erosion' and 'dilation' images described previously.

4. a series of additional two dimensional LUTs stored in the form of a TIFF image, each LUT summarising a consistency measurement. The following LUTs are available:

    1. `date_ERODIL_LUT_NORM_tile.tif` for the norm of the displacement vector between adjacent puzzle pieces;
    2. `date_ERODIL_LUT_ADX_tile.tif` for the absolute value of the horizontal displacement between adjacent puzzle pieces;
    3. `date_ERODIL_LUT_ADY_tile.tif` for the absolute value of the vertical displacement between adjacent puzzle pieces;
    4. `date_ERODIL_LUT_COOR_tile.tif` for the radiometric correlation coefficient between the adjacent puzzle pieces.

    For example, the value at coordinates x-y in the LUT `date_ERODIL_LUT_NORM_tile.tif` indicates that the norm of the mean displacement vector between the images indexed in the file `tile.tif_list.txt` by the values x and y. Similarly to the `dsr` LUTs described in Sec. 2.2, these 4 2-dimensional LUTs are stored in the directory `ALL`.

3 Coverage 1

Two mosaics products are available depending on whether data ROIs (DROIs) or their restriction to the country or countries the images were delivered for (CROIs) are used. The first mosaic maximises the use of the delivered imagery without taking into account the country/countries of origin of the input images. It provides a mosaic with as little gaps and clouds as possible but at the expense of geometric accuracy because the georeferencing specifications of an an image overlapping other countries than those it was delivered for are not necessarily met in these latter countries. The mosaic based on CROIs address this issue by considering only those parts of the image that fall within the country or

the countries the image was delivered for (but at the expense of not using all available imagery).

In the Secs.3.1–3.3, results are presented according to the three categories described in Sec. 2 and using CROIs. Section 3.4 shows examples of differences obtained when considering DROIs instead of CROIs.

3.1 Base layers

Base layers described in Sec. 2.1 are not represented in this report. Indeed, the degree of overlap images have already been illustrated for each coverage in [10] while examples of point-wise minimum and maximum compositions have been presented in [8]. Examples of point-wise maximum compositions were also presented in [6] for a visual assessment of the quality of the proposed cloud detection algorithm.

3.2 Mosaic layers

Mosaic layers described in Sec. 2.2 are displayed in Figs. 1–6 in the following order: mosaic of multispectral imagery, labelled decision regions, and their mapping to sensor type as well as the year, month, and week of acquisition (thanks to the LUTs stored in the ASCII `dsr` files). Figure 7 and 8 shows a series of examples highlighting that seam lines largely follow salient image structures. The following colour codes are used for displaying increasing overlap levels: red (i.e., only one image available), green, blue, yellow, magenta, cyan, and white for overlap levels greater or equal to 0. It can be observed that clouds occurring in the mosaic largely fall in regions where there is no overlap (see last 2 examples of Fig. 7). Note that, in some situations, there may be unfortunate image combinations leading to cut lines following ROI borders. Figure 9 illustrates 2 such cases. In the top case, there are too many overlapping images without clouds so that precedence was given to the few images not overlapping any other image (red regions in the image of overlaps). In the bottom case, an image contains so much clouds (bottom right section) so that it stops being used as soon as another image becomes available.

3.3 Quality layers

A direct graphical representation at European scale of the quality layers described in Sec. 2.3 is impossible given the scale of the figures presented in this document (2 pixel thick lines are not visible). Therefore, for visual purposes only, the measured quantities were expanded from the boundaries of the puzzle pieces using a dilation by an octagon of size 11 [4]. The resulting pictures obtained for the two main quality measures are displayed in Figs. 10 and 11: norm of the mean displacement vector and radiometric correlation coefficient. The majority of norms of the mean displacement vectors is less than half a pixel. However, in some areas, displacements between pairs of adjacent puzzle pieces well exceed this threshold value. For example, many neighbouring pieces in the Balkans reveal displacement vectors with a norm exceeding half or even a full pixel. It is also noticeable that most puzzle pieces in Iceland are separated by displacement vectors whose norms exceed one pixel. The correlation coefficient mapped in Fig. 11 have been calculated for the TOA values of the mid infrared

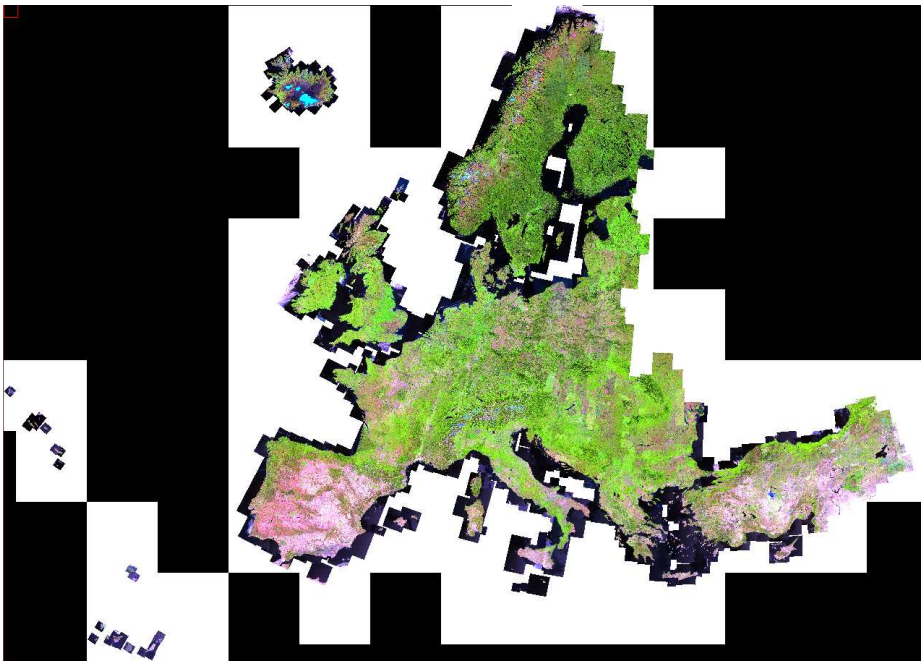

Figure 1: Top of atmosphere mosaic of first coverage based on CROIs and matching the labelled decision regions displayed in Fig. 2.

Figure 2: Labelled decision regions for the first coverage based on CROIs (1944 images used in mosaic out of 2004).

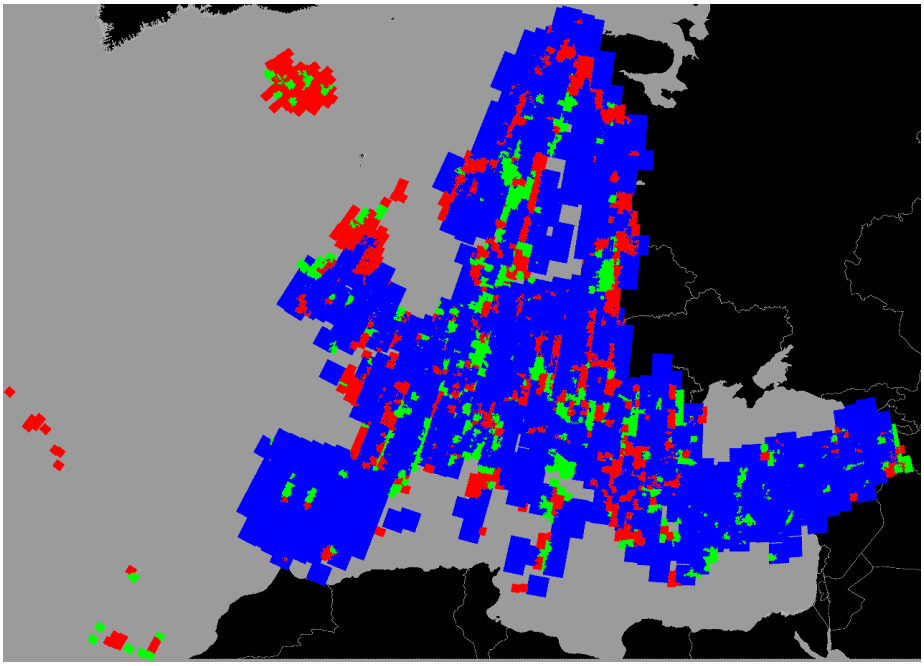

Figure 3: Decision regions of Fig. 2 mapped to sensor of image associated with each decision region of Fig. 2: red for SPOT-4, green for SPOT-5, blue for IRS-LISS.

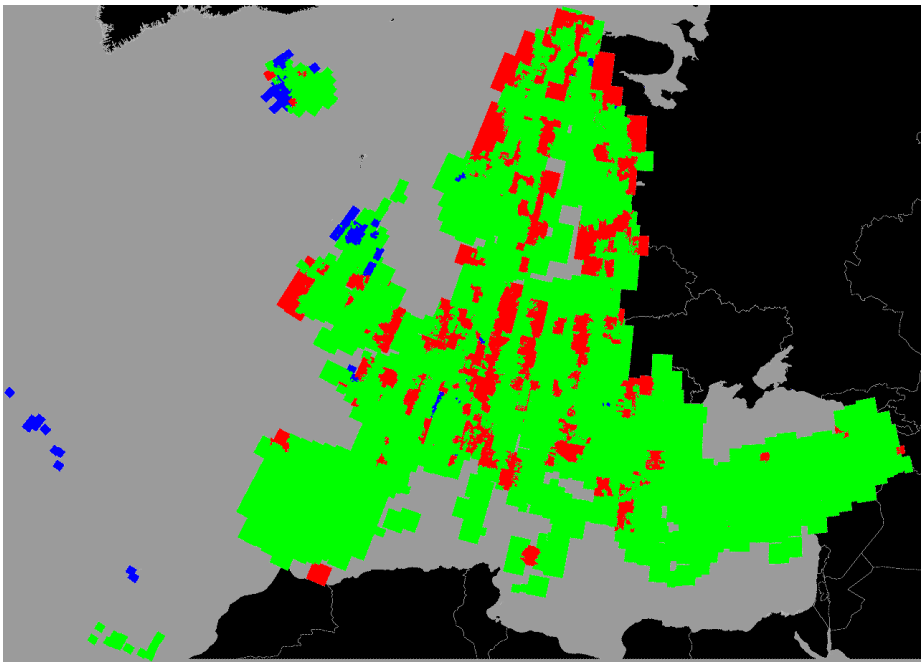

Figure 4: Decision regions of Fig. 2 mapped to year of acquisition of image associated with each decision region of Fig. 2: red for 2005, green for 2006, and blue for 2007.

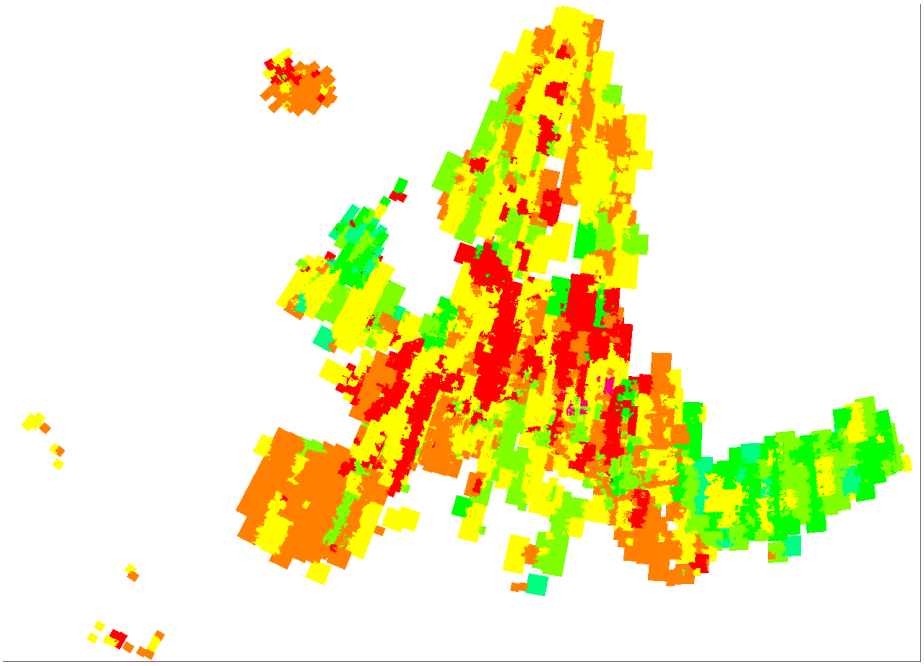

Figure 5: Decision regions of Fig. 2 mapped to month of acquisition of image associated with each decision region of Fig. 2. Month are coded using colour wheel, e.g., green for April, yellow for June, red for August, and magenta for October (see month LUT description on page 4 for the colour of each month).

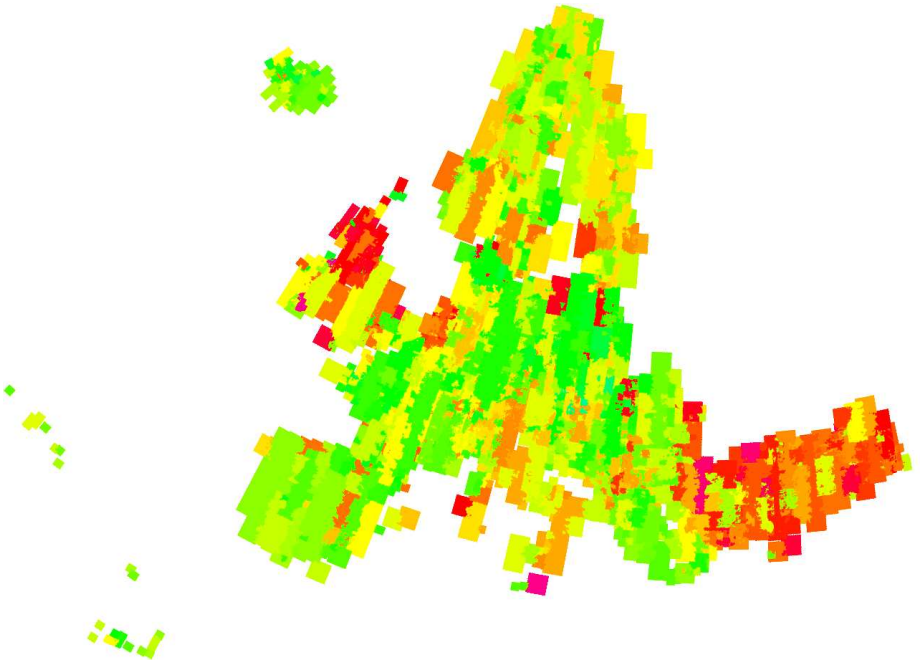

Figure 6: Decision regions of Fig. 2 mapped to week of acquisition of image associated with each decision region of Fig. 2.

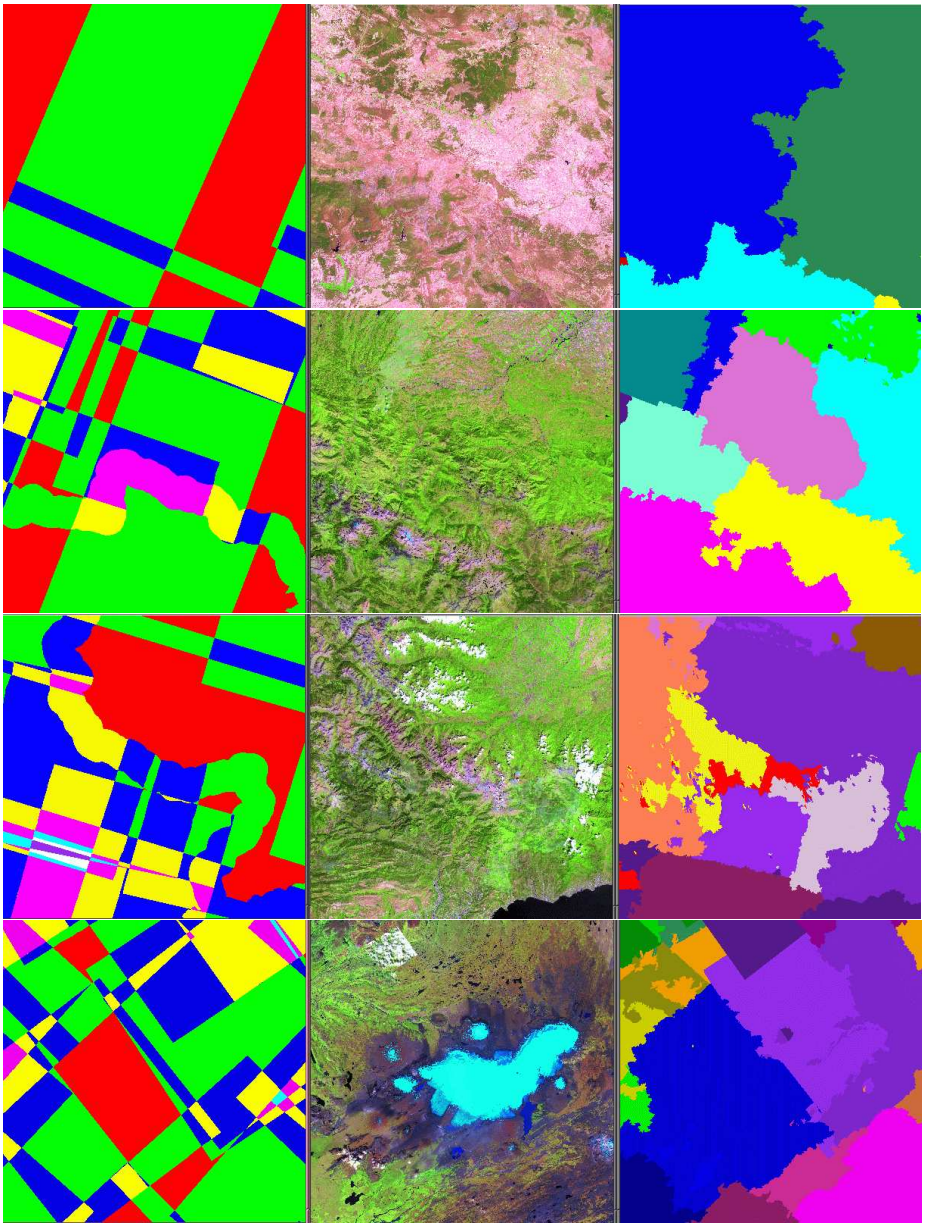

Figure 7: Gallery of overlap level images (left column), the resulting mosaic (middle column), and the underlying labelled decision regions (right column).

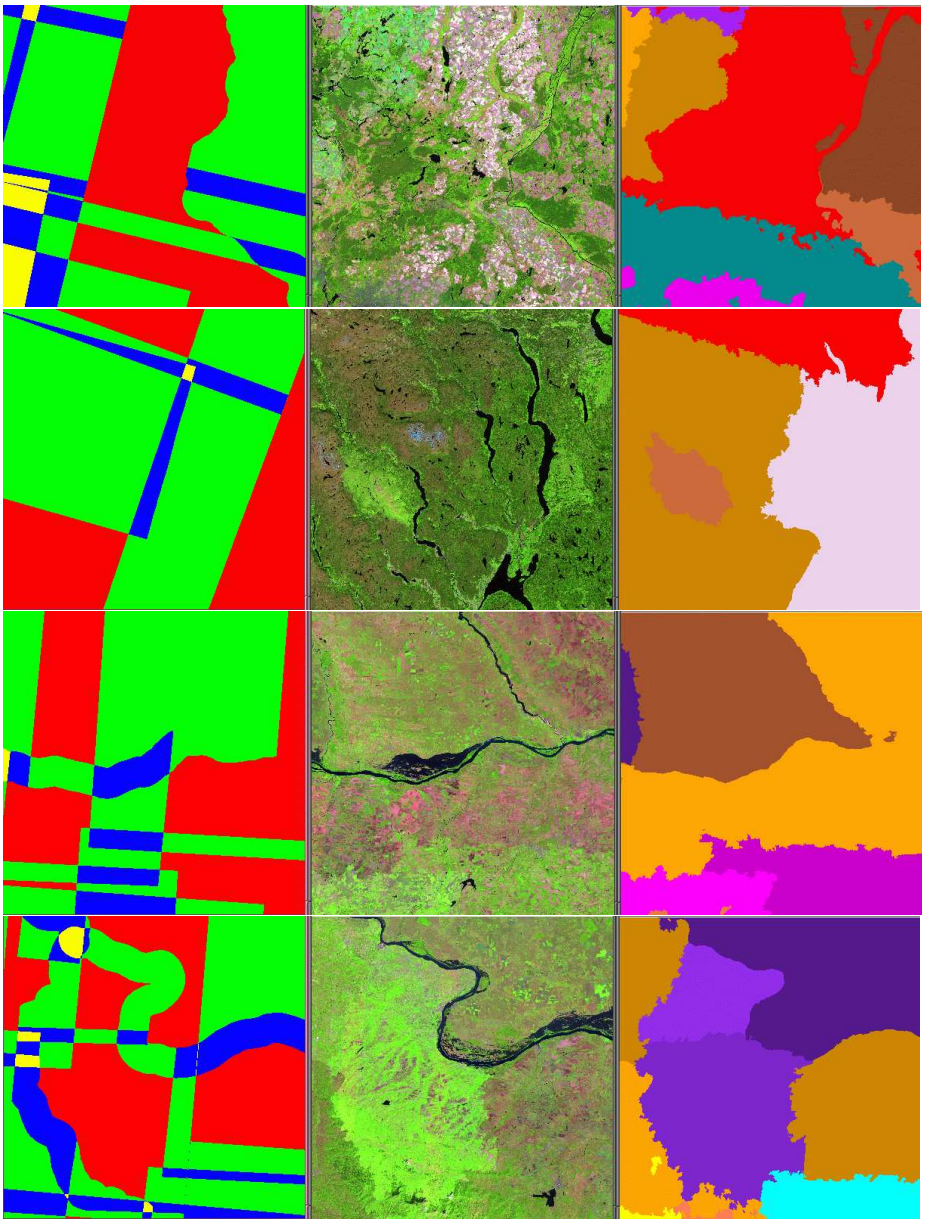

Figure 8: Gallery of overlap level images (left column), the resulting mosaic (middle column), and the underlying labelled decision regions (right column).

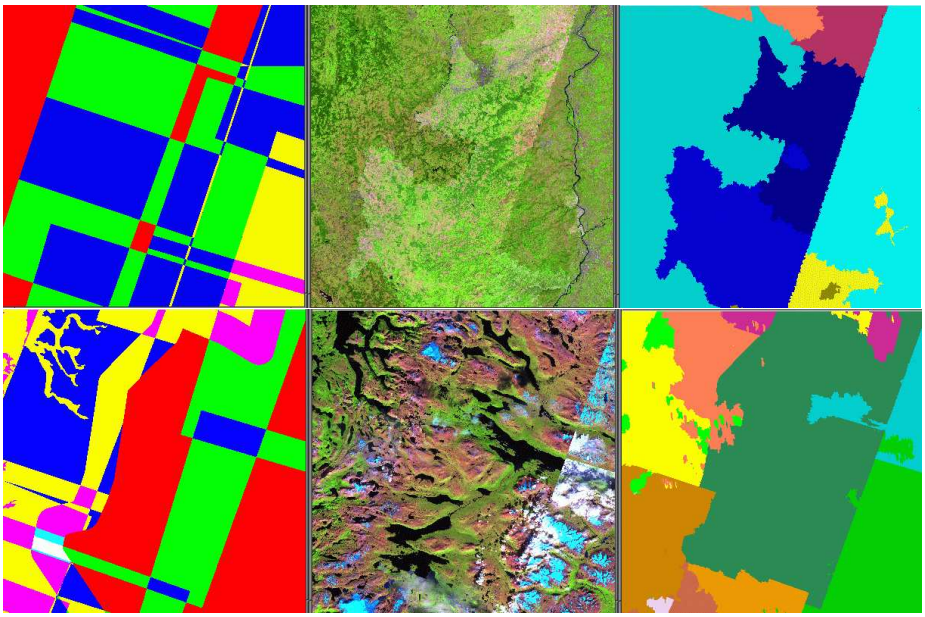

Figure 9: Gallery of overlap level images (left column), the resulting mosaic (middle column), and the underlying labelled decision regions (right column). In these examples, straight ROI borders are visible.

band. One of the largest regions with correlation coefficient above 0.9 is the Iberian peninsula owing to a coverage with almost one sensor (IRS) and during more or less the same period of the year as revealed by Figs. 3 and 5 respectively.

3.4 From CROIs to DROIs

The same information layers are available for the mosaic of coverage 1 based on DROIs instead of CROIs. Figure 12 shows examples where the results obtained for DROIs depart from those obtained for CROIs. In some fewer cases, regions not covered by CROIs (i.e., imagery delivered for a country missing part of that country) is covered by imagery delivered by neighbouring countries and therefore are visible in the mosaic based on DROIs. This happens for instance for the Greek Megisti Island that is not included in the set of imagery delivered for Greece but appears in an image delivered for Turkey given its location near the coast of Turkey.

The norm of the displacement vector measured within the overlapping domains of the image pair meeting at the decision region boundaries and calculated on the basis of DROIs is mapped in Fig. 13 for all decision regions of the first coverage and bases on DROIs. The comparison of this figure with the one obtained for CROIs shows that larger displacements are sometimes obtained near the boundaries of the participating boundaries (see for example red line between Ireland and Northern Ireland occurring in Fig. 13 but not in Fig. 10. This was expected given the relative geometric consistency measurements for both CROIs and DROI summarised in [9].

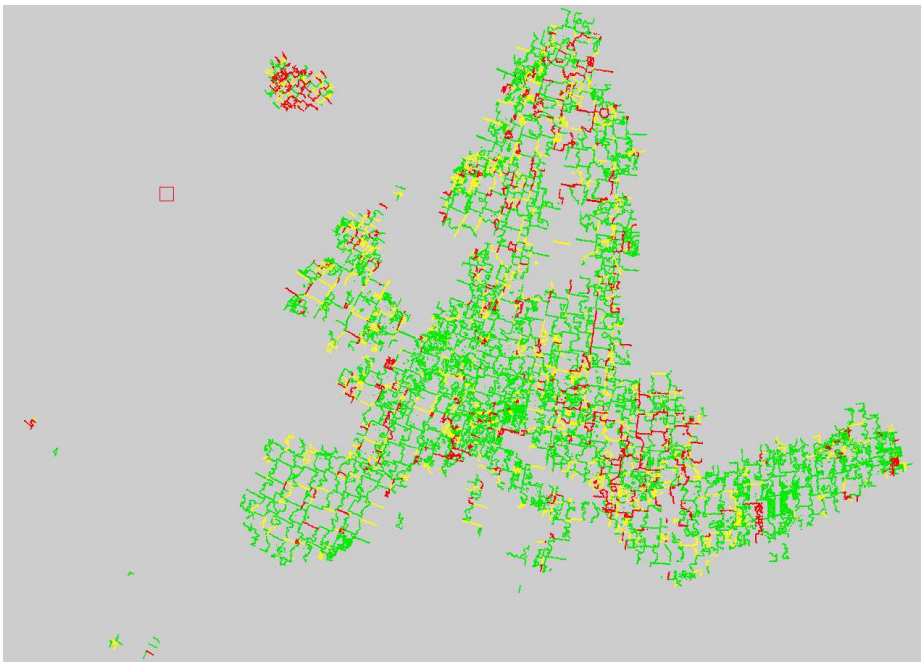

Figure 10: Norm d of the mean displacement vector measured within the overlapping domains of the image pair meeting at the decision region boundaries of Fig. 2. Green: $d \leq 0.5$ pixel. Yellow: $0.5 < d \leq 1.0$ pixel. Red: $d > 1$ pixel.

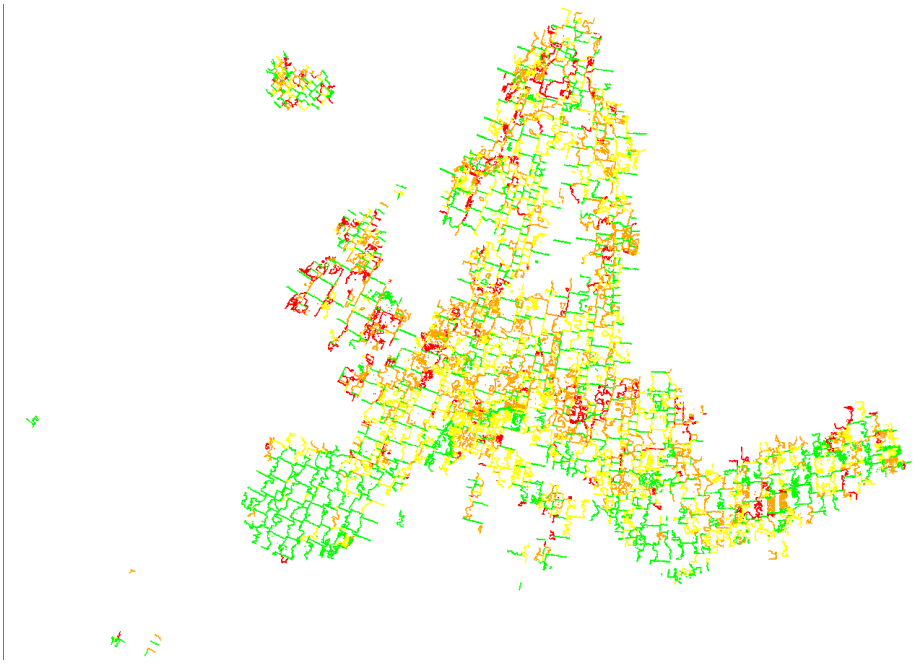

Figure 11: Radiometric correlation coefficient ρ measured within the overlapping domains of the image pair meeting at the decision region boundaries of Fig. 2. Green: $\rho > 0.9$. Yellow: $0.75 < \rho \leq 0.9$. Orange: $0.5 < \rho \leq 0.75$. Red: $\rho \leq 0.5$.

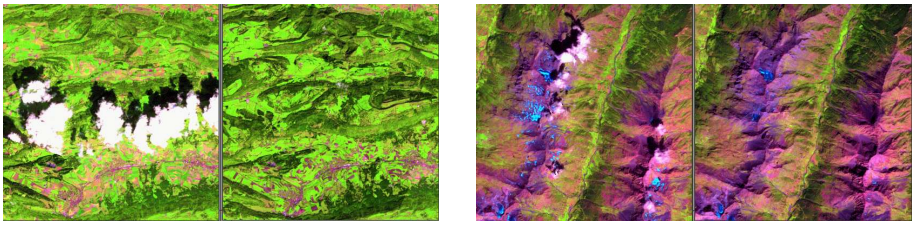

Figure 12: Coverage 1 mosaics: two examples of differences between CROI and DROI based mosaics. Right: near the border between Switzerland and France. Left: near the border between Italy and France.

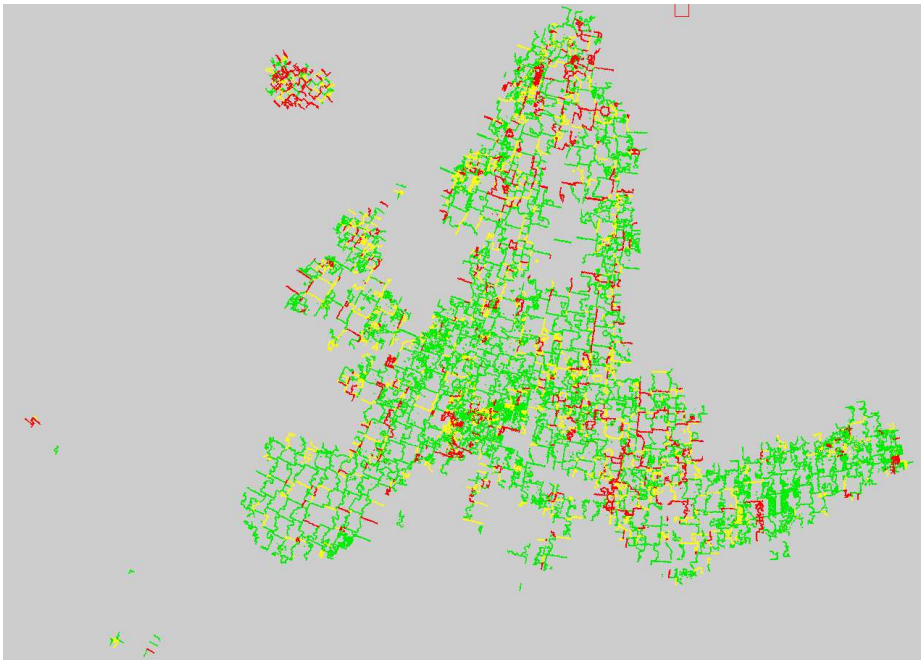

Figure 13: Norm d of the mean displacement vector measured within the overlapping domains of the image pair meeting at the DROI based decision region boundaries of the first coverage. Green: $d \leq 0.5$ pixel. Yellow: $0.5 < d \leq 1.0$ pixel. Red: $d > 1$ pixel. Compare with Fig. 10.

4 Coverage 2

The same comments as those made for coverage 1 applies. Results obtained for the mosaic layers based on DROIs are displayed in Figs. 15–19.

5 Conclusion

Morphological compositing [5] and its extension to the parallel order independent processing of large image data sets [8] enabled the automatic creation of a range of top-of-atmosphere reflectance mosaics minimising the visual detection of the cuts between overlapping images. Because morphological compositing permits the suppression of specific structures not appearing in at least one of the available images, clouds and their shadows were minimised thanks to their prior detection by the algorithm described in [6]. In summary, visually pleasing yet physically meaningful mosaics were created without applying cosmetic operations such as histogram balancing. That is, the values of the generated mosaics are comparable across the data set since they are given in TOA reflectance values. In addition, if necessary, it is possible to know from which image originates every single pixel of the mosaic. Beyond web mapping applications, all these properties make the mosaic with its accompanying information layers an added value product for subsequent analysis at the pan-European level.

Future research will aim at producing absolute rather than relative radiometric consistency measurements and, subsequently, map the TOA reflectance values to ground reflectance values by applying atmospheric correction procedures.

References

[1] A. Annoni, editor. *European Reference Grids*, volume EUR 21494 EN. European Commission, Joint Research Centre, 2005. URL `http://www.ec-gis.org/sdi/publist/pdfs/annoni2005eurgrids.pdf`.

[2] C. Bielski and P. Soille. Order independent image compositing. *Lecture Notes in Computer Science*, 3617:1076–1083, 2005. doi:`10.1007/11553595_132`.

[3] J.-F. Rivest, P. Soille, and S. Beucher. Morphological gradients. *Journal of Electronic Imaging*, 2(4):326–336, October 1993. doi:`10.1117/12.159642`.

[4] P. Soille. *Morphological Image Analysis: Principles and Applications*. Springer-Verlag, Berlin Heidelberg New York, 2nd edition, 2003.

[5] P. Soille. Morphological image compositing. *IEEE Transactions on Pattern Analysis and Machine Intelligence*, 28(5):673–683, May 2006. doi:`10.1109/TPAMI.2006.99`.

[6] P. Soille. IMAGE-2006 Mosaic: Cloud detection on SPOT-4 HRVIR, SPOT-5 HRG, and IRS-LISS III. Technical report, European Commission, Joint Research Centre, 2008.

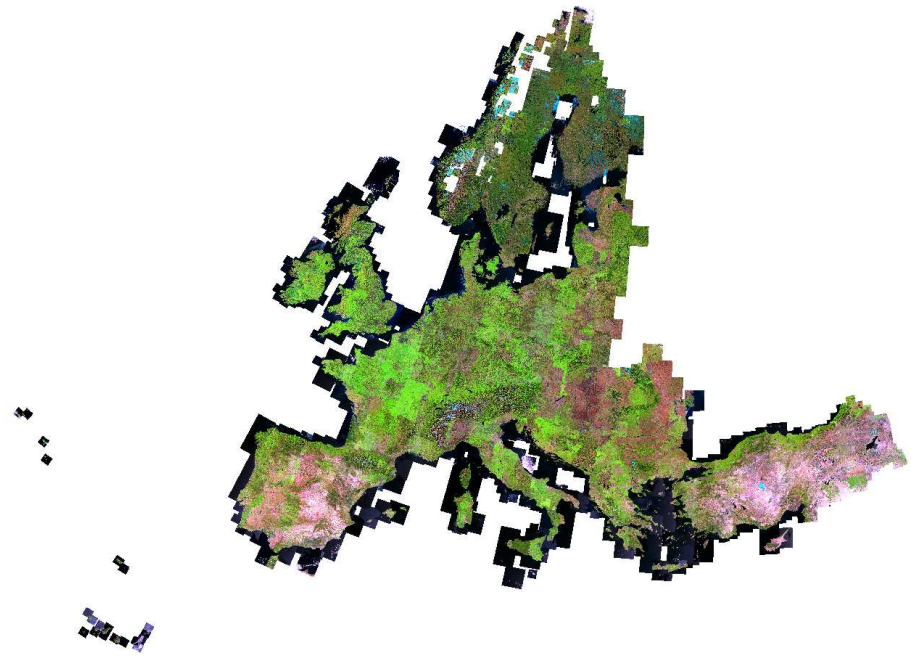

Figure 14: Top of atmosphere mosaic of second coverage based on DROIs and matching the labelled decision regions displayed in Fig. 15.

Figure 15: Labelled decision regions for the second coverage based on CROIs (1493 image used in mosaic out of 1561).

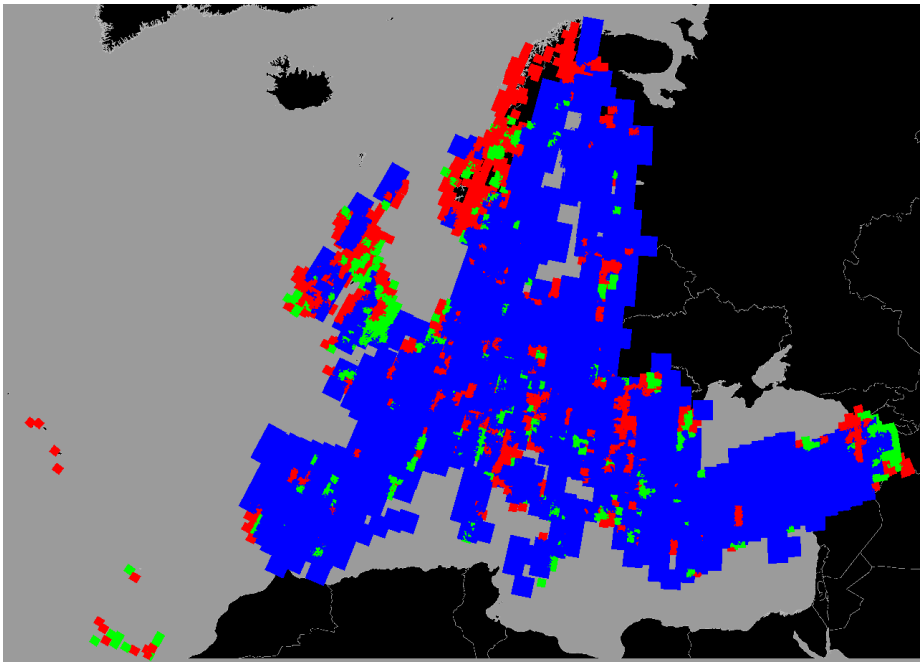

Figure 16: Decision regions of Fig. 15 mapped to sensor of image associated with each decision region of Fig. 15: red for SPOT-4, green for SPOT-5, blue for IRS-LISS.

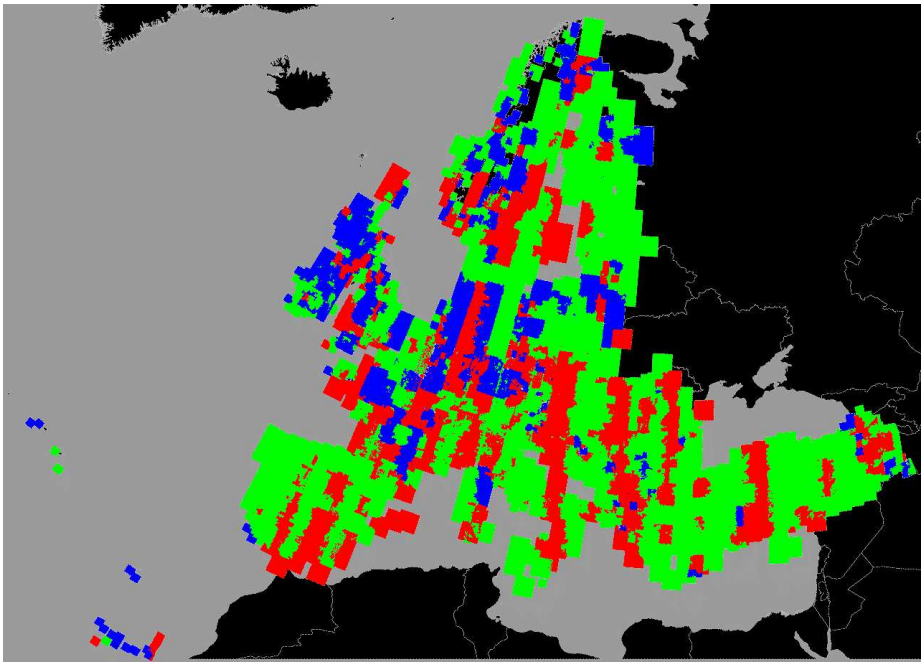

Figure 17: Decision regions of Fig. 15 mapped to year of acquisition of image associated with each decision region of Fig. 15: red for 2005, green for 2006, and blue for 2007.

Figure 18: Decision regions of Fig. 15 mapped to month of acquisition of image associated with each decision region of Fig. 15. Month are coded using colour wheel, e.g., green for April, yellow for June, red for August, and magenta for October (see month LUT description on page 4 for the colour of each month).

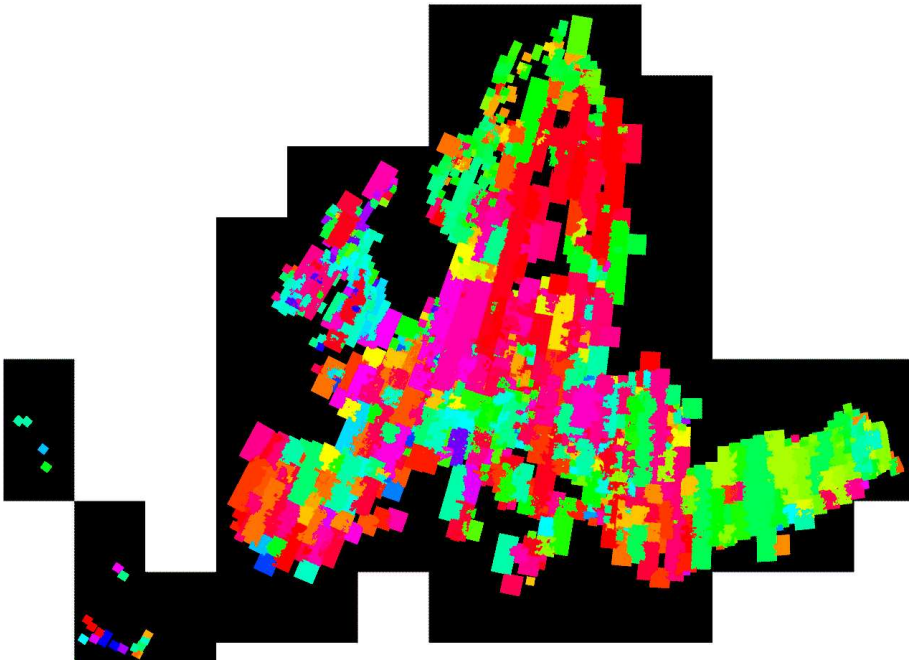

Figure 19: Decision regions of Fig. 15 mapped to week of acquisition of image associated with each decision region of Fig. 15.

[7] P. Soille and C. Bielski. IMAGE-2006 Mosaic: Data ingestion and organisation. Technical report, European Commission, Joint Research Centre, 2008.

[8] P. Soille and C. Bielski. Automatic seam line delineation of large image data sets. *IEEE Transactions on Geoscience and Remote Sensing*, 2008. In preparation.

[9] P. Soille and J. Grazzini. IMAGE-2006 Mosaic: Geometric and radiometric consistency of input imagery. Technical report, European Commission, Joint Research Centre, 2008. In preparation.

[10] P. Soille, C. Bielski, and J. Nowak. IMAGE-2006 Mosaic: Analysis of image footprints —v.1.0—. Technical report, European Commission, Joint Research Centre, May 2008.

[11] P. Strobl. Organising a shared raster data repositery for LMNH and SDI units. Technical report, European Commission, Joint Research Centre, 2008.

European Commission

EUR 23636 EN – Joint Research Centre – Institute for Environment and Sustainability
Title: IMAGE-2006 Mosaic: Product Description
Author: Pierre Soille and Conrad Bielski
Luxembourg: Publications Office of the European Union
2011 – 19 pp. – 21.0 x 29.7 cm
EUR – Scientific and Technical Research series – ISSN 1831-9424 (online), 1018-5593 (print)
ISBN 978-92-79-20960-4
doi:10.2788/51244

Abstract
This report describes the IMAGE-2006 mosaic products. Each product consists of a range of information layers grouped into three categories: base layers, mosaic layers, and quality layers. A mosaic product is available for each coverage and data/country region of interest combination.

The mission of the JRC is to provide customer-driven scientific and technical support for the conception, development, implementation and monitoring of EU policies. As a service of the European Commission, the JRC functions as a reference centre of science and technology for the Union. Close to the policy-making process, it serves the common interest of the Member States, while being independent of special interests, whether private or national.

JRC
EUROPEAN COMMISSION

LB-NF-23636-EN-N

Publications Office